



HAL
open science

Green process technology for peroxydicarboxylic acids: Estimation of kinetic and dispersion parameters aided by RTD measurements: Green synthesis of peroxydicarboxylic acids

Sébastien Leveueur, Johan Wärnå, Kari Eränen, Tapio Salmi

► To cite this version:

Sébastien Leveueur, Johan Wärnå, Kari Eränen, Tapio Salmi. Green process technology for peroxydicarboxylic acids: Estimation of kinetic and dispersion parameters aided by RTD measurements: Green synthesis of peroxydicarboxylic acids. *Chemical Engineering Science*, 2011, 66 (6), pp.1038-1050. 10.1016/j.ces.2010.12.005 . hal-02151572

HAL Id: hal-02151572

<https://normandie-univ.hal.science/hal-02151572v1>

Submitted on 27 Jan 2022

HAL is a multi-disciplinary open access archive for the deposit and dissemination of scientific research documents, whether they are published or not. The documents may come from teaching and research institutions in France or abroad, or from public or private research centers.

L'archive ouverte pluridisciplinaire **HAL**, est destinée au dépôt et à la diffusion de documents scientifiques de niveau recherche, publiés ou non, émanant des établissements d'enseignement et de recherche français ou étrangers, des laboratoires publics ou privés.

Green process technology for peroxy-carboxylic acids: estimation of kinetic and dispersion parameters aided by RTD measurements: green synthesis of peroxy-carboxylic acids

Sébastien Leveneur^{a,b}, Johan Wärnå^a, Kari Eränen^a, Tapio Salmi^a*

^aLaboratory of Industrial Chemistry and Reaction Engineering, Process Chemistry Centre, Åbo Akademi University, Biskopsgatan 8, FI-20500 Åbo/Turku, Finland.

^bLSPC-Laboratoire de Sécurité des Procédés Chimiques, INSA Rouen, BP08, Avenue de l'Université, 76801 Saint-Étienne-du-Rouvray, France.

Tel: +33 2 32 95 66 54; Fax: +33 2 32 95 66 96; E-mail: sebastien.leveneur@insa-rouen.fr

ABSTRACT

Synthesis of peroxypropionic and peroxyacetic acids from hydrogen peroxide and their carboxylic acids was carried out in a continuous fixed-bed reactor, demonstrating the concept of green process technology: biodegradable chemicals are made with the aid of heterogeneous catalysts. This reactor was constructed with several sampling locations along its length, allowing a better kinetic investigation. A profound study of the mean residence time distribution (RTD) was performed to analyze the behaviour of the flow pattern at different liquid flow rates and catalyst loadings by using step and impulse methods with different tracer molecules. It was found that impulse experiments with HCl as a tracer is the most reliable method to study the RTD because of this tracer does not interact with the catalyst. Based on the RTD study, it was demonstrated that the temperature (in the range 30-60°C) and the catalyst distribution inside the reactor do not affect the

flow pattern, but the ratio of the catalyst mass-to-liquid ratio affects the mean residence time and the liquid dispersion. Furthermore, it was shown that the presence of axial dispersion is negligible when the average particle diameter is less than 1.38 mm, e.g., the Péclet number exceeds 100. The kinetic study was carried out at different mean residence times (from 10 to 55 min), at different wet catalyst loadings (from 25 to 49 g) and reactor temperatures (from 30 to 60°C). Mathematical models comprising kinetic and dispersion parameters were developed to compare the estimated parameters obtained from the continuous fixed-bed reactor with the ones obtained from a batch reactor.

Keywords: Peroxycarboxylic acid, Kinetics, Fixed-bed reactor, Residence Time Distribution, Mathematical modelling, Cation exchange resin catalysts

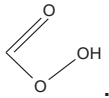
1. Introduction

The environmental impact and the safety aspects for the production of chemicals are the two main issues to ensure the sustainability of industrial production. Preventing the formation of waste products, suppressing the energy consumption, designing safer processes, utilizing non-toxic and non-hazardous chemicals, and optimizing the productivity are the main concerns of all the chemical companies. The concept of “Green Chemistry” introduced in the 1990’s has provided methods and tools to take into account these issues for the scientific and industrial community. Later on, the concept of “green process technology” has been developed, emphasising the importance of continuous technology, use of non-toxic heterogeneous catalyst and driving at biodegradable products.

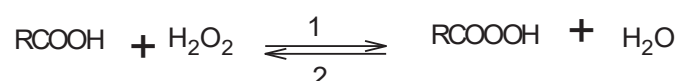
Oxidation reactions are fundamental in industry, but many of these reactions are carried out by using conventional heavy-metal oxidants, which form toxic waste, application of nitric acid which form the greenhouse gas N_2O ; and utilization of molecular oxygen, which requires safety precautions and could cause over-oxidation. According to Noyori (2007), an elegant way to surmount these problems is the use of aqueous hydrogen peroxide, as the oxidant hydrogen peroxide is a powerful oxidant.

Among all these reactions carried out in the presence of hydrogen peroxide, the perhydrolysis of carboxylic acid can be an example of the application of green chemistry and green process technology. The reaction product is a peroxy-carboxylic acid.

The market volume of peroxy-carboxylic acids can be estimated to be some 10000 tonnes worldwide (Rüsch et al., 2002). Three domains of application can be distinguished: disinfecting agent, bleaching agent and as an intermediate in fine chemistry. All these applications are based on the oxidative properties of these

compounds, due to the chemical bond .

Several routes of the synthesis of peroxy-carboxylic acids are available, such as oxygenation of the parent aldehyde (Phillips et al., 1958) or carboxylic acid (Cantieni, 1937). The reaction of carboxylic acid perhydrolysis is described by the following equation:



This reaction is reversible and requires the presence of an enhancing chemical species, an acid catalyst, since the carboxylic acid itself is usually a too weak acid to promote the reaction velocity.

Traditionally, this reaction is catalyzed by mineral acids, such as sulfuric acid leading to several drawbacks such as corrosion, threat for the environment and catalyst separation. Cation exchange resins have been found to be the most adequate catalysts for this reaction (Leveneur et al., 2009a, 2009b, 2009c;

Hawkinson and Schitz, 1957; Musante et al., 2000). The great benefit is that the resins do not decompose the peroxide species. However, most of the previous studies reported in the open literature have been carried out in a batch reactor.

The research efforts concerning the perhydrolysis reactions in continuous reactors in the presence of heterogeneous catalysts are scarce (Saha et al., 2003). The objective of this paper is to demonstrate that the development of a continuous process concept based on the use of heterogeneous catalysts for manufacture of peroxy-carboxylic acids is possible, and to provide a comparison with the kinetics obtained in batch and continuous modes. The second objective is to provide a profound study of the flow pattern by using different methods (step and impulse) and different tracer molecules. The final aim is to develop a model including kinetic and dispersion effects.

2. Experimental section

2.1. Apparatus and experimental procedures

The chemical reaction and the residence time distribution (RTD) experiments were carried out in the same continuous reactor. However, the injection procedures were different. The reactor was set up in diagonal to ease the sampling and prevent back-mixing phenomenon.

Perhydrolysis reaction

A jacketed catalytic fixed-bed reactor consisting of catalyst layers and inert materials (for sampling) was used. The reactor was operated in the upflow mode to enhance the catalyst wetting, and put in a diagonal position. By inclining the reactor in such position, one could expect the formation of dead spaces or bypassing, which were not detected during the residence time distribution study. The main reasons for such setup were to ease the sampling, to diminish backmixing compared to a vertical reactor operating in upflow mode and to avoid the trapping of gas in case of peroxides decomposition (compared to a horizontal position). Samples were withdrawn from different positions in the reactor. Amberlite IR-120 was used as the heterogeneous catalyst. Fig. 1 presents a schematic view of the experimental setup. The length of the reactor was 60 cm and the internal diameter was 1.45 cm.

Here Figure 1.

In a first stage, a mixture of carboxylic acid (propionic acid: Acros, 99 wt.% or acetic acid: J.T.Baker 99-100 wt.%) and hydrogen peroxide solution (Merck, 30 wt.%) were mixed together in a separate storage vessel placed in a water bath. After 30 minutes (time to reach the desired reaction temperature), this mixture was fed to the continuous reactor through a pump. The experimental data for the kinetics modelling were obtained after three hours of time-on-stream, to safely operate under steady state conditions. Different amounts of catalyst and inert materials were used in the experiments as illustrated by Scheme 1.

Here Scheme 1.

Table 1 shows the experimental conditions used while Table 2 shows the properties of quartz inert material and Amberlite IR-120 resin catalyst.

Here Table 1.

Here Table 2.

Residence time distribution

Pulse and step experiments were used to determine the residence time distribution (RTD) in the fixed-bed reactor. In general, the tracer molecule should have a similar structure to that of the reactant and the product molecules, without interfering with the catalyst. For the sake of comparison, acetic acid, propionic acid, hydrogen peroxide and hydrochloric acid were used as tracers.

In case of pulse experiments, around 1-2 g of the solution at 0.02 M of HCl, 1 or 5 M of propionic acid was introduced at the inlet of the reactor during 2-5 s. The tracer experiments were carried out at two different temperatures: 30°C and 50°C, and different flow rates. Step experiments were performed with two pumps connected to two batch vessels. One of the vessels contained the tracer dissolved in de-ionized water and the other one only deionised water. In both cases, the concentration of the tracer was followed on-line by conductivity, and the data were recorded 5 s intervals.

2.2. Chemical analysis

The liquid phase was analyzed off-line by titration with Greenspan and Mackellar methods (Greenspan and Mackellar, 1948). The concentration of hydrogen peroxide was determined by titration using a standard solution of ammonium cerium sulfate (0.1 N). The concentrations of carboxylic and peroxy-carboxylic acids were determined by titration with an automatic titrator (Metrohm 751 GPD Titrino) using a standard solution of sodium hydroxide (0.2 N).

2.3. Catalyst properties

The ion exchange resins were washed with deionised water and filtered before introducing into the fixed-bed reactor. The properties of Amberlite IR-120 are summarized in Table 3. It is a cation exchange resin with a styrene-divinyl benzene matrix bearing sulfonic acid groups. The catalyst was used in the form of beads.

Here Table 3.

The tubular reactor was filled with wet catalyst, i.e., in a first stage the native catalyst was washed with deionised water, and then filtrated.

3. Results and discussions

3.1 Residence time distribution

The study of the flow pattern (RTD) is an important issue of this work. The flow pattern investigation was mainly carried out with the reactor 4 (the presence of only one layer of catalyst) to find the most adequate method to measure RTD.

3.1.1 Pulse experiments

The pulse experiments were carried out with HCl and propionic acid.

HCl as a tracer

Hydrochloric acid was used because it is a strong electrolyte and does not interfere with the resin. Due the small concentration of the HCl solution along the reactor, the following relationship was used to determine its concentration at the outlet versus time,

$$\sigma = \lambda c \quad (1)$$

where σ is the measured conductivity [$\text{S}\cdot\text{m}^{-1}$], c is the concentration [$\text{mol}\cdot\text{m}^{-3}$] and λ [$\text{S}\cdot\text{m}^2\cdot\text{mol}^{-1}$] is the molar conductivity.

Fig. 2 displays the E-curves recorded at different flow rates at the reactor outlet (reactor 4). The function E is defined as:

$$E(t) = \frac{C(t)}{\text{Area under concentration of pulse versus time}} \quad (2)$$

$$= \frac{C(t)}{\sum C(t)\Delta t}$$

Here Fig.2.

Fig. 2 shows that the distribution is symmetric. The mean residence time \bar{t} was calculated from the experimental data as follows:

$$\bar{t} = \frac{\sum_i t_i C_{\text{pulse},i} \Delta t_i}{\sum_i C_{\text{pulse},i} \Delta t_i} \quad (3)$$

On the other hand, the mean residence time is related to the volumetric flow rate (F)

$$\bar{t} = \frac{V_L}{F} \quad (4)$$

where V_L represents the void volume of the tube reactor, i.e. the liquid volume. Fig. 3 represents the flow rate versus the inverse of the mean residence time at 50°C. The mean residence time was obtained from Eq. (3). The plot is a straight line, as reported.

Here Fig. 3

In the case of the reactor 4, the flow pattern is equal to 34.22 ml as depicted by Fig. 3. Levenspiel (1999) has introduced the dimensionless group $\frac{D}{uL}$, where D [$\text{m}^2.\text{s}^{-1}$] is the axial dispersion coefficient, L the length of the vessel [m] and u the superficial velocity [$\text{m}.\text{s}^{-1}$]. This parameter is called vessel dispersion number, and measures the extent of the axial dispersion. The reciprocal value of $D/(uL)$ is called Péclet number (Pe).

Thus, $\frac{D}{uL} \rightarrow 0$ negligible dispersion, hence plug flow and $\frac{D}{uL} \rightarrow \infty$ large dispersion, hence mixed flow.

The parameter $D/(uL)$ can be determined from the experimentally recorded mean residence time (\bar{t}^2) and variance (Var).

$$\frac{\text{Var}}{\bar{t}^2} = 2 \left(\frac{D}{uL} \right) \quad (5)$$

The amount of catalyst and inert material was similar between reactors 1 and 4, but their distributions along the reactor were different. Fig. 4 shows the evolution of \bar{t} at different flow rates for reactors 1 and 4.

Here Fig. 4.

Table 4 shows the value of the parameter $D/(uL)$ and the Pé number for each reactor at different flow rates. It can be concluded that the axial dispersion effect is rather negligible in both cases, since the Péclet number obtains a high value, in most cases exceeding 100.

Here Table 4.

Fig. 4 and Table 4 confirm that the flow pattern does not depend on the distribution of the catalyst and the inert material. The RTD measurements carried out at 30°C gave the same value of \bar{t} and D/uL ; so the flow pattern does not depend on the temperature within the temperature range of 30-50°C.

Here Fig. 5.

Fig. 5 presents the evolution of the mean residence time \bar{t} with the flow rate. It is a clear tendency that increasing the catalyst loading leads to a decrease of the liquid volume in the reactor. Indeed, by decreasing the amount of catalyst loading, the average diameter \bar{d}_p increases because the amount of glass balls increases.

In case of reactors 1, 2 and 4, the axial dispersion effect was negligible during the impulse measurement carried out with the HCl solution. However, in case of reactor 3 (lowest catalyst loading), axial dispersion was noticeable. Fig. 6 shows the E-curves for different flow rates, and the presence of a tail in the curve is visible at different flow rates.

Here Fig. 6.

The parameter D/uL is less than 0.01 for reactor 1, 2 and 4, but in the case of reactor 3 this parameter is slightly higher as shown by Table 5.

Here Table 5

According to the experimental setup, the measurement was done in closed conditions. Thus, to evaluate $D/(uL)$, the following equation valid for axial dispersion model was used:

$$\frac{\sigma^2}{\bar{t}^2} = 2\left(\frac{D}{uL}\right) - 2\left(\frac{D}{uL}\right)^2 [1 - e^{-uL/D}] \quad (6)$$

According to Chander et al. (2001), the Pé number is influenced by the size of the particles inside a fixed-bed reactor. During their experiments, they have noticed that axial dispersion is significant with particle diameter higher than 1.1 mm. By calculating the average particle diameter (Table 8), one can notice that the presence of axial dispersion appears when the diameter of the particle is bigger, i.e. the diameter of the particle is equal to 1.38 mm for reactor 3 and lower than 1.14 mm for the other reactors.

Propionic acid as a tracer

The steric hindrance of H_2O_2 and HCl molecule is similar, but not for propionic or acetic acid. Propionic acid is a weaker electrolyte than HCl, for that reason a more concentrated solution than HCl solution was used. Due to the high concentration of the carboxylic acid solution used, Eq. (1) cannot be used for the interpretation of the primary data. However, the exit age distribution curve can be calculated by considering the intensity of the signal as follow:

$$E = \frac{\sigma(t)}{\text{area under conductivity versus time}} \quad (7)$$

$$= \frac{\sigma(t)}{\sum \sigma(t)\Delta t}$$

Two concentrations of propionic acid were used, 1 and 5 M. The results obtained with a solution of 1 M of propionic acid gave better results, i.e., the distribution is close to Gaussian. In view of the journal space limitation, only the E-curves for concentration at 1 M is shown (Fig. 7).

Here Fig. 7.

By using propionic acid as a tracer molecule, the estimated volume of liquid in the reactor is between 60-63 ml, which is higher than the one determined by HCl solution. The difference of RTD for HCl and propionic acid is due to the fact that propionic acid adsorbs to some extent on the active site of the catalyst (Leveneur et al., 2009d), and thus takes a longer time to be released from the reactor.

Table 6 displays the value of the dispersion parameters calculated with RTD experiments performed at different propionic acid concentrations. One can notice that the estimated value of $Pé$ is low, which might be due to the adsorption of propionic acid on the resin.

Here Table 6.

3.1.2 Step response experiments

Step response experiments were used to check whether there are any phenomena of hysteresis by using HCl or propionic acid as a tracer molecule. Positive and negative step experiments were carried out.

Step response experiments with HCl

The F-curve obtained from the relation:

$$F = \frac{C_{\text{step}}}{C_{\text{max}}} \quad (8)$$

where C_{max} is the tracer concentration at steady state.

Here Fig. 8.

Fig. 9 displays the evolution of the mean residence time by using positive and negative step methods.

Here Fig. 9.

Fig. 9 indicates that there is a difference between the positive and negative step, essentially at high flow rates.

Step response experiments with propionic and acetic acid

Step experiments with a solution of acetic acid concentrated at 1.2 mol/l and propionic acid at 0.98 mol/l were carried out. The presence of a hysteresis effect was higher than with hydrochloric acid, which suggests that carboxylic acids are not the more adequate molecules to determine RTD in the present case.

3.1.3 Conclusions from the RTD studies

Fig. 10 depicts the flow rate versus the mean residence time with different methods (step and pulse) and tracer molecules.

Here Fig. 10.

Fig. 10 shows that the RTD profile given by step experiments with a solution of propionic and acetic acid at 7 wt.% are similar. This is due the similarity of both molecules regarding the adsorption properties, and confirms that these molecules cannot be used as tracers to determine the RTD.

The measurement of the residence time distribution by impulse method with carboxylic acid gave different results than the pulse experiment with hydrochloric acid or the step method with carboxylic acid. Due to the fact that the adsorption of carboxylic acid on the resins can interfere with a real measurement of the RTD,

the mean residence \bar{t} was calculated based on impulse method determined with hydrochloric acid.

Table 7 shows the values of the $D/(uL)$ and Péclet number at 50°C at different flow rates using impulse method with HCl.

Here Table 7.

Table 7 confirms that axial dispersion in reactor 3 should be taken into account. For this reason, two different models were developed one by taking into account the axial dispersion effect and the other one based on the plug flow concept exclusively.

3.2 Estimation of the pressure drop

The pressure drop for a fluid flowing through a column packed with solid particles is commonly evaluated by means of Ergun equation:

$$\frac{\Delta P}{\Delta L} = A \frac{\varepsilon_{RP}^2}{(1-\varepsilon_{RP})^3} \frac{\mu_f}{(\bar{d}_p)^2} u_f + B \frac{\varepsilon_{RP}}{(1-\varepsilon_{RP})^3} \frac{\rho_f}{\bar{d}_p} u_f^2 \quad (9)$$

where,

ε_{RP} : fraction of solid in the reactor,

$1 - \varepsilon_{RP}$ void fraction in reactor,

$\bar{d}_p = \frac{6\varepsilon_{RP}}{A_s}$, mean diameter particle and A_s is external surface area of particle by

volume of reactor, m^2/m^3 , μ_f : fluid viscosity, Ns/m^2 , ρ_f : fluid density, kg/m^3 and u_f : superficial velocity, m/s.

Water is the solvent in the system (around 50-55 wt. %), for that reason water viscosity and density were used in Eq. (9). The external surface area of the particle was calculated based on the data from Table 3 and the nominal diameter of the wet Amberlite IR-120 were used (0.5 mm). Table 8 shows the fraction of solid in the reactor, parameter A_s , mean diameter of particle for each reactor.

Here Table 8.

According to Trambouze and Euzen (2002), in case of liquid phase system, the parameters A and B could change according to the nature of the liquid. According

to Villermaux (1993), if $\frac{Re_p}{\epsilon_{RP}} < 500$, then A and B are equal to 150 and 1.75,

respectively. The Reynolds number for the particle is defined as:

$$Re_p = \frac{\bar{d}_p u_f \rho_f}{\mu_f} \quad (10)$$

The value of Re_p varies between 0.06 and 0.8 for the different reactors; thus, the parameter A and B can be fixed to be equal to 150 and 1.75, respectively.

By using Eq. (9), it was observed that the pressure drop is negligible, e.g., lower than 10^{-5} mBar/m in the superficial velocity range 9 (from $4 \cdot 10^{-5}$ to $4 \cdot 10^{-5}$ m/s) applied during the experiments.

3.3 Mass transfer effects

Several methods exist in the literature to estimate the mass transfer coefficient k_D in case of external mass transfer. The mass flux N_D between the bulk phase and the surface of the catalyst is expressed as

$$N_D = k_D(C_b - C_s) \quad (11)$$

where k_D is the mass transfer coefficient, C_b and C_s are the concentrations in the bulk and at the outer surface of the catalyst, respectively.

The coefficient k_D ($\text{m}\cdot\text{s}^{-1}$) (Villermoux, 1993) can be estimated by calculating the Sherwood number (Sh) defined as

$$\text{Sh} = \frac{k_D \bar{d}_p}{D} = 2 + 1.8 \text{Re}_p^{1/2} \text{Sc}^{1/3} \quad (12)$$

where Sc is the Schmidt number defined as

$$\text{Sc} = \frac{\mu_f}{\rho_f D} \quad (13)$$

and D is the molecular diffusion coefficient, estimated by using the Wilke-Chang equation (Salmi et al., 2010). The molar volumes of the dissolved components and the liquid viscosity are included in the Wilke-Chang equation. The molar volumes were calculated from the atomic increments of Le Bas. At 30°C, the molecular diffusion coefficients of the different compounds present in the mixture are quite close ($1.29 - 3.32 \cdot 10^{-9} \text{m}^2\cdot\text{s}^{-1}$).

Villermoux (1993) has defined the coefficient f_e to determine the influence of the external mass transfer:

$$f_e = \frac{\bar{r}L}{k_D C_b} = \frac{C_b - C_s}{C_b} \quad (14)$$

where \bar{r} is the initial observed reaction rate ($\text{mol}\cdot\text{m}^{-3}\cdot\text{s}^{-1}$), and L is defined as the ratio V_P/A_P . If f_e is less than 5 %, then the external mass transfer is negligible.

Another way to estimate the mass transfer coefficient k_D is to use the correlation proposed by Satterfield-Chilton-Colburn:

$$j_D = \frac{k_D Sc^{2/3}}{u_f} \quad (15)$$

In case of a liquid-phase reaction and if $0.006 < Re_p < 55$ (Villermaux, 1993), the parameter j_D is defined as:

$$j_D = \frac{1.09}{(1 - \varepsilon_p) Re_p^{0.67}} \quad (16)$$

The viscosity and density of water was used in the calculation. For the sake of simplicity, Table 9 summarizes the values of the different numbers used for estimating the mass transfer coefficient k_D and the value of f_e in case of reactor 1 for the perhydrolysis of propionic acid. The molecular diffusion of propionic acid was used to calculate k_D from Eq.(12).

Here Table 9.

Table 9 shows that the parameter f_e is lower than 5 %, which proves the absence of external mass transfer. Furthermore, both values of f_e , i.e., calculated from Sh or j_D , are similar, confirming the previous conclusion. By using this methodology for the different reactors, no external mass transfer limitation was noticed for the synthesis of PAA or PPA.

To estimate the importance of internal mass transfer, Villermaux (1993) has introduced the parameter ϕ'_s defined as,

$$\phi'_s = \frac{\bar{r}L^2}{D_e C_s} \quad (17)$$

where $L = V_p/A_p$,

If ϕ'_s is lower than 0.1, internal mass transfer is negligible. In our case, $C_s = C_b$ because there is no external mass transfer limitation. Indeed, when ϕ'_s is equal to 0.1, then deviation caused by internal diffusion limitation is about 6% for a first-order reaction. The effective diffusion coefficient D_e is defined as, $D_e = \frac{\varepsilon_p}{\tau} D$, where ε_p is the porosity and τ is the tortuosity factor of the material. In case of Amberlite IR-120, the porosity is equal to 0.5 and the tortuosity factor was estimated to be 2.2 (Leveneur et al., 2009d). The molecular diffusion coefficient D of propionic acid was estimated by using the Wilke-Chang equation.

The value of ϕ'_s for the synthesis of peroxypropionic acid performed with reactor 1 was estimated to 0.02 at 30°C, showing the absence of internal mass transfer limitation. This tendency was observed for the different experiments carried out during this study, i.e., the absence of internal mass transfer.

3.4 Mass balance of the system

The pressure drop, evaluated by Ergun equation; external and internal mass transfer phenomena, evaluated by several correlations (Trambouze and Euzen, 2002), were found to be negligible. Thus, based on the evidence provided in previous section the pseudo-homogeneous model was applied to the fixed-bed reactor. The mass balance of a component (i) is written as follows:

$$\dot{n}_{i,\text{in}} + \left(-D_a \frac{\partial C_i}{\partial l} A_l \right)_{\text{in}} + r_{i,\text{tot}} \Delta V_L = \dot{n}_{i,\text{out}} + \left(-D_a \frac{\partial C_i}{\partial l} A_l \right)_{\text{out}} + \frac{\partial n_i}{\partial t} \quad (18)$$

where the area element is defined by

$$A_l = 2\pi r \Delta r$$

The axial dispersion coefficient is defined by $D_a = \varepsilon D$, where ε is the liquid hold-up defined by $\varepsilon = V_L / V$, V being the total volume of the reactor. The differences can be written by the operator Δ :

$$\Delta \left(D_a \frac{\partial C_i}{\partial l} A_l \right) + r_{i,\text{tot}} \Delta V_L = \Delta \dot{n}_i + \frac{\partial n_i}{\partial t} \quad (19)$$

The volume element is $\Delta V = A_l \Delta l$ and the amount of substance can be written as $n_i = c_i \Delta V_L = c_i \varepsilon \Delta V$. By dividing Eq.(19) by $2\pi r \Delta r \Delta l$ and assuming D_a constant, Eq.(19) becomes

$$D_a \frac{\Delta \left(\frac{\partial C_i}{\partial l} \right)}{\Delta l} + r_{i,\text{tot}} \frac{\varepsilon \Delta V}{2\pi r \Delta r \Delta l} = \frac{\Delta \dot{n}_i}{2\pi r \Delta r \Delta l} + \frac{\partial n_i}{2\pi r \Delta r \Delta l \partial t} \quad (20)$$

The relationship between superficial velocity w and length of reactor is $w = \frac{l}{t}$.

Thus, Eq.(20) becomes:

$$\frac{D_a}{w^2} \frac{\Delta \left(\frac{\partial C_i}{\partial \bar{t}} \right)}{\Delta \bar{t}} + r_{i,\text{tot}} \varepsilon = \frac{\Delta \dot{n}_i}{2\pi \Delta r \Delta l} + \frac{\partial n_i}{2\pi \Delta r \Delta l \partial t} \quad (21)$$

The following expression for the molar flow is valid:

$$\Delta \dot{n}_i = \Delta(c_i w) 2\pi \Delta r \quad (22)$$

Then,

$$\frac{\Delta \dot{n}_i}{2\pi \Delta r \Delta l} = \frac{\Delta(c_i w)}{\Delta l} = \frac{\Delta(c_i)}{\Delta \bar{t}} \quad (23)$$

Letting $\Delta \bar{t} \rightarrow 0$, the mass balance becomes:

$$\frac{D_a}{w^2} \frac{\partial^2 c_i}{\partial \bar{t}^2} + r_{i,\text{tot}} \varepsilon = \frac{\partial c_i}{\partial \bar{t}} + \varepsilon \frac{\partial c_i}{\partial t} \quad (24)$$

At steady state regime, there is no accumulation, $\frac{\partial c_i}{\partial t} = 0$ and the equation is

simplified to

$$\frac{D_a}{w^2} \frac{\partial^2 c_i}{\partial \bar{t}^2} + r_{i,\text{tot}} \varepsilon = \frac{\partial c_i}{\partial \bar{t}} \quad (25)$$

The Danckwerts boundary conditions were applied for differential equation,

at the reactor inlet $c_{oi} = c_i - \frac{D_a}{w^2} \frac{dc_i}{d\bar{t}}$ at $\bar{t} = 0$

at the reactor outlet $\frac{dc_i}{d\bar{t}} = 0$ at \bar{t}

In case of absence of axial dispersion and at steady-state, Eq.(19) leads to :

$$r_{i,\text{tot}} \Delta V_L = \Delta \dot{n}_i \quad (26)$$

The volume element is $\Delta V = A_l \Delta l$, superficial velocity is $w = \frac{l}{\bar{t}}$ and by using

Eq.(22), we get,

$$\varepsilon_{i,\text{tot}} = \frac{dc_i}{dt} \quad (27)$$

i.e., the plug flow model.

3.5 Kinetic expression for perhydrolysis

In a previous paper of our group (Leveneur et al., 2009d), the kinetics of peroxy-carboxylic acid synthesis was described in detail. Perhydrolysis is a reversible reaction governed by the value of the equilibrium constant K^C .

Based on the experimental data obtained from a batch reactor, an Eley-Rideal mechanism was assumed to operate, but the autoprotolysis of carboxylic acid itself gives some contribution to the overall reaction rate.

Here Fig. 11.

From Fig. 11, it should be noticed that the mechanism can be divided into two parts: the homogeneous part r_{hom} due to the protolysis of carboxylic acids producing hydroxonium ions, which act catalytically; and the heterogeneous part r_{het} due to the sulphonic groups on the resins. The peroxy-carboxylic acid is a much weaker acid than the corresponding carboxylic acid. Therefore, the acid-catalytic effect of the peroxy-carboxylic acid is not included in the scheme. The details of the calculation of the homogeneously catalyzed part are given in the previous article (Leveneur et al., 2008). The total rate r_{tot} of the reaction is the sum of the rates of the reactions 2 and 6, in Fig.11.

$$r_{\text{tot}} = r_{\text{hom}} + r_{\text{het}} = \left[\frac{k_{\text{hom}} * \sqrt{K_{\text{CA,diss}}} * [\text{CA}] * [\text{W}]}{[\text{W}]} + \frac{k_{\text{het}} * \rho_{\text{LB}} * \text{Cap.}(4.7\text{m}\alpha\text{I/g})}{1 + K_{\text{ads,CA,PCA}}^C * ([\text{CA}] + [\text{PCA}]) + K_{\text{ads,W}}^C * [\text{W}]} \right] * \left[[\text{CA}] * [\text{HP}] - \frac{1}{K^C} * [\text{PCA}] * [\text{W}] \right] \quad (28)$$

where ρ_{LB} represents the amount of dried catalyst (kg) per volume of void (V_L) in each section of the reactor.

The concentration-based equilibrium constant K^C is defined as: $K^c = \frac{K^T}{K^\gamma}$, where K^γ represents the equilibrium ratio calculated based on the activity coefficients and K^T is the thermodynamic equilibrium constant. For the sake of simplicity, K^γ was assumed to be constant in the temperature range 30-60°C, and, the constant K^C was calculated as: $K^c = \frac{K^T}{K^\gamma}$, where K^γ was found to be equal to 0.8 (Leveneur et

al., 2009d), and K^T was determined from $\ln \frac{K^T}{K_{ref}^T} = \frac{-\Delta H_r^\circ}{R} \left(\frac{1}{T} - \frac{1}{T_{ref}} \right)$. The parameters

ΔH_r° and K_{ref}^T were estimated from a previous model for peroxyacetic and peroxypropionic acid synthesis (Leveneur et al., 2009d). The value for the adsorption coefficient of water $K_{ads,W}^C$ (equal to 0.72 at 45°C) was calculated based on the equation developed by Altiokka (2007), and $K_{CA,diss}$ (equal to $2.8 \cdot 10^{-7}$ for acetic acid and $2.2 \cdot 10^{-7}$ for propionic acid at 45°C) was estimated from Sue et al. (2004). The parameter $K_{ads,CA,PCA}^C$ was estimated by the model (Leveneur et al., 2009d).

Eq. (25) was used only in the case of reactor 3 for the synthesis of peroxyacetic acid, where the presence of axial dispersion was confirmed by the RTD measurement.

3.6 Reactor modelling results

In the sake of simplicity, the liquid hold-up was assumed to be constant in the different part of the reactors. By making this assumption, one can calculate the \bar{t} of each section of the reactor, and define a global axial dispersion parameter.

The parameter estimation was carried out by a special software Modest for simulation and parameter estimation (Haario, 2001). The objective function θ was minimized by using Simplex and Levenberg-Marquardt algorithms. This objective function was defined as follows $\theta = \sum (c_i - \hat{c}_i)^2$ where c_i is the experimental concentration and \hat{c}_i is the estimated concentration. The concentrations of CA, PCA and H₂O₂ were included in the objective function with equal weights.

In this model, two parameters were estimated by regression analysis: k_{ave} and Ea with the reference temperature fixed at 45°C. The temperature dependence of the rate constant was described by a modified Arrhenius equation:

$$k = k_{ave} \exp\left(\frac{-Ea}{R} \left(\frac{1}{T} - \frac{1}{T_{ave}}\right)\right) \quad (29)$$

where $k_{ave} = Ae^{-\left(\frac{Ea}{RT_{ave}}\right)}$, T_{ave} is the average temperature of the experiments. The goal of this modification is to suppress the correlation between the frequency factor and the activation energy during the parameter estimation.

The coefficient of explanation R^2 of the kinetic models is defined as follows:

$$R^2 = 1 - \frac{\sum (c_i - \hat{c}_i)^2}{\sum (c_i - \bar{c}_i)^2} \quad (30)$$

where c_i is the experimental concentration, \hat{c} is the estimated concentration and \bar{c} is the mean value of the observed concentrations.

3.6.1 Absence of axial dispersion – plug flow model

The generation rates of the chemical compounds are combined to the mass balances valid for the continuous reactor (Eq. 27),

$$\begin{aligned}\frac{d[\text{PA}]}{d\bar{t}} &= -\varepsilon r_{i,\text{tot}} \\ \frac{d[\text{PPA}]}{d\bar{t}} &= +\varepsilon r_{i,\text{tot}} \\ \frac{d[\text{H}_2\text{O}_2]}{d\bar{t}} &= -\varepsilon r_{i,\text{tot}} \\ \frac{d[\text{H}_2\text{O}]}{d\bar{t}} &= +\varepsilon r_{i,\text{tot}}\end{aligned}$$

This ordinary differential equation system was solved with backward difference method implemented in the software Odessa, which is a part of the Modest package. Fig. 12 shows the modelling results obtained in case of negligible axial dispersions.

Here Fig. 12.

One should remember that the reactor was divided into different sections, which were alternatively fed with inert materials and catalysts. By assuming that the liquid hold-up was the same along the reactor, it was possible to determine the mean residence time \bar{t} at the different section of the continuous reactor.

The explanation coefficient for this model is 99.40 %. Table 10 gives the values of the estimated parameters.

Here Table 10.

Here Fig. 13

Fig. 13 represents the contour plot of E_a versus k_{ave} demonstrating a well-pronounced minimum, and the parameters are rather well defined. The average rate constant and activation energy for the synthesis of peroxypropionic acid in batch reactor were estimated to be equal to $k_{ave} = 0.91 \cdot 10^{-3} \text{ l.mol}^{-1}.\text{s}^{-1}$ and $E_a = 51.4 \text{ kJ.mol}^{-1}$, respectively. One can notice that the kinetic parameters are in fairly good agreement.

3.6.2 Modelling in the presence of axial dispersion

According to the RTD measurement, the presence of axial dispersion was noticed in the experiments carried out with reactor 3. By combining the generation rates with the mass balance Eq. (25), the following set of differential equations is obtained

$$\frac{D_a}{w^2} \frac{\partial^2 [AA]}{\partial \bar{t}^2} - r_{\text{tot}} \mathcal{E} = \frac{\partial [AA]}{\partial \bar{t}}$$

$$\frac{D_a}{w^2} \frac{\partial^2 [PAA]}{\partial \bar{t}^2} + r_{\text{tot}} \mathcal{E} = \frac{\partial [PAA]}{\partial \bar{t}}$$

$$\frac{D_a}{w^2} \frac{\partial^2 [H_2O_2]}{\partial \bar{t}^2} - r_{\text{tot}} \mathcal{E} = \frac{\partial [H_2O_2]}{\partial \bar{t}}$$

$$\frac{D_a}{w^2} \frac{\partial^2 [H_2O]}{\partial \bar{t}^2} + r_{\text{tot}} \mathcal{E} = \frac{\partial [H_2O]}{\partial \bar{t}}$$

These differential equations were transformed to ordinary differential equation using central finite difference method. The axial dispersion coefficient D_a and the kinetic parameters such as rate constant k_{ave} and E_a were estimated by regression. Fig. 14 shows the modelling results obtained in presence of axial dispersion.

Here Fig. 14.

The explanation coefficient for this model became 99.20 %, and the Table 11 gives the value of the estimated parameters and the standard error values.

Here Table 11.

For this modelling, the estimated parameters were further checked by parameter sensitivity analysis plots using the Markov Chain Monte Carlo (MCMC) method (Fig. 15). Fig. 15 indicates that the parameters are really well identified.

Here Fig. 15.

8. CONCLUSIONS

The goal of this paper was to demonstrate the feasibility and the possibility to scale-up the production of peroxy-carboxylic acid (PAA and PPA) from carboxylic acid and hydrogen peroxide in a continuously operating fixed-bed reactor, in the presence of a heterogeneous catalyst. The experimental setup allows to take samples at different locations in the reactor. Thus, the experimental concentration profile can be verified with modelling.

Residence time distribution measurements were carried out by step and pulse methods and with different tracer molecules. The experiments carried out by pulse method using HCl as a tracer gave a better description of the flow pattern. It was observed that neither the reactor temperature nor the catalyst distribution inside the reactor has an influence on the flow pattern. The increase of the average diameter of the particles led to an increase of the mean residence time, since the void fraction of the bed increased. In case of experiments carried out with a low catalyst loading (i.e., reactor 3), axial dispersion phenomenon cannot be neglected, but has to be taken into account in the modelling.

By using the Ergun equation, it was found that the pressure drop is negligible in this study. Several correlations confirmed the fact that external and internal mass transfer are absent under the experimental conditions used. Based on these conclusions, a steady-state pseudo-homogeneous model with and without axial dispersion was developed to estimate the kinetic parameters at the temperature range of 30-50°C. The validity of this model is correct for a water concentration

range of 27.80-48.7 M, a carboxylic acid concentration range of 5.10-5.90 M, a hydrogen peroxide concentration of 6.10-7.00 M, a flow rate of 0.6-3.6 ml.min⁻¹ and different catalyst loadings were used, from 25.0 to 48.7 g. The kinetic model developed is able to fairly describe the system in the presence and absence of axial dispersion.

AKNOWLEDGEMENTS

The financial support from the Åbo Akademi Forskningsinstitut and the Finnish Graduate School in Chemical Engineering (GSCE) are gratefully acknowledged. This work is part of the activities at the Åbo Akademi Process Chemistry Centre (PCC) within the Finnish Centre of Excellence Programme (2006-2011) by the Academy of Finland.

NOTATION

A	interfacial area [m ²]
A _s	external surface area of the particle by volume, m ² /m ³
c	concentration [mol.l ⁻¹]
D	axial dispersion coefficient [m ² .s ⁻¹]
D	molecular diffusion coefficient [m ² .s ⁻¹]
De	effective diffusion coefficient [m ² .s ⁻¹]
Ea	activation energy [J.mol ⁻¹]
F	volumetric flow rate of the fluid [ml/min]
f _a	coefficient to evaluate the influence of external mass transfer
ΔH _r ^o	standard reaction enthalpy [kJ.mol ⁻¹]
j _D	$\frac{k_D Sc^{2/3}}{u_f}$
K ^c	equilibrium constant, based on concentrations
K ^T	thermodynamic equilibrium constant, based on activities
K ^y	equilibrium constant, based on activity coefficients
K	adsorption coefficient [l.mol ⁻¹]
k	rate constant [l.mol ⁻¹ .s ⁻¹]
k _D	mass transfer coefficient [m/s]
L	vessel length [m]
N	flux [mol.m ⁻² .s ⁻¹]

N_D	mass flux between the bulk phase and the catalyst surface [$\text{mol}\cdot\text{m}^{-2}\cdot\text{s}^{-1}$]
n	amount of substance [mol]
\dot{n}	flow of amount of substance [$\text{mol}\cdot\text{s}^{-1}$]
R	gas constant [$\text{J}\cdot\text{K}^{-1}\cdot\text{mol}^{-1}$]
R^2	coefficient of explanation [%]
r_i	generation rate
\bar{r}_{obs}	observed reaction rate [$\text{mol}\cdot\text{m}^{-3}\cdot\text{s}^{-1}$]
T	temperature
w	superficial velocity [$\text{m}\cdot\text{s}^{-1}$]
V	volume
Var	variance
V_L	liquid volume
\bar{t}	mean residence time [s]

Greek letters

ε	fraction of liquid in the reactor
ε_{RP}	fraction of solid in the reactor
ε_P	particle porosity
θ	objective function
λ	molar conductivity [$\text{S}\cdot\text{m}^2\cdot\text{mol}^{-1}$]
μ_f	fluid viscosity [Ns/m^2]
ρ_f	fluid density [kg/m^3]
σ	conductivity [$\text{S}\cdot\text{m}^{-1}$]

Subscripts and superscripts

o	initial
ref	reference state
[i]	concentration of a component <i>i</i> [mol.l ⁻¹]
ave	average
b	bulk phase
i	component index
f	fluid
L	liquid

Abbreviations

AA	acetic acid
PA	propionic acid
PAA	peroxyacetic acid
PPA	peroxypropionic acid
RTD	residence time distribution

Dimensionless groups

Pé	Péclet number, $(uL)/D$
Re	Reynolds number for the reactor $d_{\text{reactor}}u_f\rho_f/\mu_f$
Re _p	Reynold number for the particle $d_p u_f \rho_f / \mu_f$
Sh	Sherwood number, $\frac{k_D \bar{d}_p}{D}$
Sc	Schmidt number, $\frac{\mu_f}{\rho_f D}$
φ_s'	Modified Thiele modulus, $\frac{\bar{r}L^2}{D_e C_S}$

REFERENCES

Altiokka, M.R., 2007. Kinetics of hydrolysis of benzaldehyde dimethyl acetal over Amberlite IR-120. *Ind. Eng. Res.* 46, 1058-1062.

Cantieni, R., 1937. Photochemical peroxide formation. VII. Oxidation of acetic, propionic, butyric and isovaleric acids by means of molecular oxygen in ultraviolet light. *Zeitschrift fuer Wissenschaftliche Photographie, Photophysik und Photochemie.* 36, 90-95.

Chander, A., Kundu, A., Bej, S. K., Dalai, A. K., Vohra D. K., 2001. Hydrodynamic characteristics of cocurrent upflow and downflow of gas and liquid in a fixed bed reactor. *Fuel*, 80(8), 1043-1053.

Greenspan, F.P., Mackellar, D.G., 1948. Analysis of aliphatic per acids. *Anal. Chem.* 20, 1061-1063.

Haario, H., 2001. *MODEST-User's Guide*. Profmath Oy, Helsinki.

Hawkinson, A.T., Schitz, W.R., 1957. Improvements in or relating to the oxidation of aliphatic carboxylic acids to peracids. GB776758.

Leveneur, S., Salmi, T., Murzin, D. Yu., Estel, L., Wärnå, J., Musakka, N., 2008. Kinetic Study and Modeling of Peroxypropionic Acid Synthesis from Propionic Acid and Hydrogen Peroxide using Homogeneous Catalysts. *Ind. Eng. Chem. Res.*, 47(3), 656-664.

Leveneur, S., Murzin, D. Yu., Salmi, T., 2009. Application of linear free-energy relationships to perhydrolysis of different carboxylic acids over homogeneous and heterogeneous catalysts. *J. Mol. Catal. A Chem.* 303, 148-155.

Leveneur, S., Murzin, D. Yu., Salmi, T., Mikkola, J.-P., Kumar, N., Eränen, K., Estel, L., 2009. Synthesis of peroxypropionic acid from propionic acid and hydrogen peroxide over heterogeneous catalysts. *Chem. Eng. J.* 147, 323-329.

Leveneur, S., Wärnå, J., Salmi, T., Murzin, D. Yu., Estel, L., 2009. Interaction of intrinsic kinetics and internal mass transfer in porous ion-exchange catalysts: green synthesis of peroxydicarboxylic acids. *Chem. Eng. Sci.* 64 (19), 4104-4114.

Levenspiel, O., 1999. *Chemical Reaction Engineering*. 3rd ed., John Wiley & Sons, Inc., New York.

Musante, R.L., Grau, R.J., Baltanas, M.A., 2000. Kinetic of liquid-phase reactions catalyzed by acidic resins: the formation of peracetic acid for vegetable oil epoxidation. *Appl. Catal. A* 197(1), 165-173.

Noyori, R., 2005. Pursuing practical elegance in chemical synthesis. *Chem. Commun.* 14, 1807-1811.

Phillips, B., Starcher, P. S., Ash, B.D., 1958. Preparation of aliphatic peroxyacids. *J. Org. Chem.* 23, 1823-1826.

Rüsch gen. Klaas, M., Steffens, K., Patett, N., 2002. Biocatalytic peroxy acid formation for disinfection. *J. Mol. Catal. B-Enzym.* 19-20, 499-505.

Saha, M.S, Nishiki, Y., Furuta, T., Denggerile, A., Ohsaka, T., 2003. A new method for the preparation of peroxyacetic acid using solid superacid catalysts. *Tetrahedron Lett.* 44(29), 5535-5537.

Salmi, T.O., Mikkola, J.-P., Wärnå, J.P., 2010. *Chemical reaction engineering and reactor technology*. 1st Ed. CRC Press.

Sue, K., Ouchi, F., Minami, K., Arai, K., 2004. Determination of carboxylic acid dissociation constants to 350°C at 23MPa by potentiometric pH measurements. *J. Chem. Eng. Data.* 49 1359-1363.

Trambouze, P., Euzen, J.-P., 2002. *Les Réacteurs Chimiques*. Editions TECHNIP, Paris.

Villiermaux, J., 1993. *Génie de la Réaction Chimique*. 2nd ed., Tec&Doc Lavoisier.

FIGURES

Scheme 1. Schematic view of the catalyst loadings in the fixed-bed reactor.

Fig. 1. Experimental scheme of the continuous fixed-bed reactor for continuous peroxy-carboxylic acid production.

Fig. 2. E-curves at 30°C by using HCl as a tracer.

Fig. 3. Flow rate versus the inverse of the mean residence time at 50°C for reactor 4.

Fig. 4. Flow rate versus the inverse of the mean residence time at 50°C.

Fig. 5. Evolution of \bar{t} in different reactors.

Fig. 6. E-curves for reactor 3 at different flow rates.

Fig. 7. E-curves for reactor 4 at 50°C using a 1 M of propionic acid solution.

Fig. 8. F-curve for reactor 4 at 50°C with an HCl solution at 0.003 M.

Fig. 9. Flow rate versus \bar{t} in the reactor 4 at 50°C.

Fig. 10. Flow rate versus the reciprocal value of the mean residence time for reactor 4 at 50°C.

Fig. 11. Simplified mechanism for peroxy-carboxylic acid synthesis by Amberlite IR-120 in aqueous medium.

Fig. 12. Fit of the plug flow model to the perhydrolysis experiments of propionic acid.

Fig. 13. Contour plot for the kinetic parameters.

Fig. 14. Fit of the axial dispersion model to the perhydrolysis of acetic acid carried out with reactor 3.

Fig. 15. Plots of the parameter sensitivity analysis (MCMC).

TABLES

Table 1. Experimental matrix.

Table 2. Quartz and catalyst properties.

Table 3. Properties of Amberlite IR-120.

Table 4. Evolution of the dispersion parameter D/uL and $Pé$.

Table 5. Parameter $D/(uL)$ and Péclet number for reactor 3.

Table 6. Dispersion parameters for impulse experiments with propionic acid.

Table 7. Dispersion parameters of the different reactors at 50°C.

Table 8. Geometric parameters of the reactors.

Table 9. External mass transfer parameters for reactor 1 for propionic acid.

Table 10. Estimated parameters and values of standard errors at 45°C with R^2 : 99.40 %.

Table 11. Estimated Parameters and Values of Standard Errors at 45°C with R^2 : 99.20 %.

Table 1[Click here to download Figure: Table 1.doc](#)

Table 1. Experimental matrix.

Loading of quartz balls [g]	57.6 - 99.5
Loading of wet Amberlite IR-120 [g]	25.0 - 48.7
Flow rate [ml.min ⁻¹]	0.6-3.6
Temperature [°C]	30 - 50
[CA] ₀ [mol.l ⁻¹]	5.10-5.90
[H ₂ O ₂] ₀ [mol.l ⁻¹]	6.10-7.00
[H ₂ O] ₀ [mol.l ⁻¹]	24.80-31.40

Table 2[Click here to download Figure: Table 2.doc](#)

Table 2. Quartz and catalyst properties.

Quartz		Amberlite IR-120	
Diameter [mm]	3	Diameter [mm]	0.15-0.90
Density [kg.m ⁻³]	2687	True density [kg.m ⁻³]	1260
		Porosity	0.5

Table 3[Click here to download Figure: Table 3.doc](#)

Table 3. Properties of Amberlite IR-120.

Polymer type	Gel
Cross linking, %	8
Moisture content, % mass	45
Capacity by dry weight, meq/g	4.7
Particle size range, mm	0.9

Table 4

[Click here to download high resolution image](#)

Table 4. Evolution of the dispersion parameter D/uL and $Pé$.

	Temperature [°C]	\bar{t} [min]	$\frac{D}{uL}$	$Pé$
REACTOR 1	50	50	0.006	168
	50	28	0.007	138
	50	13	0.008	119
	50	10	0.011	91
	50	7	0.011	91
REACTOR 4	50	34	0.007	140
	50	17	0.011	90
	50	13	0.007	141
	50	10	0.007	138
	50	9	0.009	117
	50	7	0.007	137

Table 5[Click here to download Figure: Table 5.doc](#)Table 5. Parameter $D/(uL)$ and Péclet number for reactor 3.

	Temperature [°C]	\bar{t} [min]	$\frac{D}{uL}$	Pé
REACTOR 3	50	36	0.07	14
	50	18	0.06	17
	50	12	0.03	29
	50	8	0.01	70

Table 6

[Click here to download Figure: Table 6.doc](#)

Table 6. Dispersion parameters for impulse experiments with propionic acid.

	Temperature [°C]	\bar{t} [min]	$\frac{D}{uL}$	Pé
PA, 1 M	50	54	0,02	53
	50	28	0,03	33
	50	19	0,04	23
	50	15	0,05	19
	50	12	0,06	15
PA, 5 M	50	67	0,04	28
	50	35	0,05	22
	50	22	0,05	20
	50	17	0,06	17
	50	13	0,07	14

Table 7

[Click here to download high resolution image](#)

Table 7. Dispersion parameters of the different reactors at 50°C.

Flow rate [ml/min]	Reactor 1		Reactor 2		Reactor 3		Reactor 4	
	$\frac{D}{\mu\text{L}}$	Pé	$\frac{D}{\mu\text{L}}$	Pé	$\frac{D}{\mu\text{L}}$	Pé	$\frac{D}{\mu\text{L}}$	Pé
1	0.01	169	0.01	149	0.07	14	0.01	140
3	0.01	119	0.01	130	0.03	29	0.02	59
5	0.01	91	0.01	107	0.01	70	0.01	117

Table 8[Click here to download Figure: Table 8.doc](#)

Table 8. Geometric parameters of the reactors.

	ε_{RP}	A_s	$\bar{d}_p = \frac{6\varepsilon_{RP}}{A_s}[\text{m}]$
Reactor 1	0.66	3485.8	1.14E-03
Reactor 2	0.68	4431.1	9.24E-04
Reactor 3	0.64	2797.6	1.38E-03
Reactor 4	0.66	3517.2	1.12E-03

Table 9. External mass transfer parameters for reactor 1 for propionic acid

Flow rate ml/min	Sc	$\bar{\Gamma}$ mol.m ⁻³ .s ⁻¹	k_D from Sh from Eq.(12) m/s	fe from Sh	j_D	k_D from Sh from Eq.(15) m/s	fe from j_D	Re _P
2.64	619	0.77	1.26E-05	0.002	6.44	2.21E-05	0.001	0.36
1.16	619	0.77	9.12E-06	0.003	11.19	1.68E-05	0.002	0.16
0.90	619	0.77	8.32E-06	0.003	13.21	1.55E-05	0.002	0.12
0.82	619	0.77	8.03E-06	0.004	14.11	1.50E-05	0.002	0.11
0.50	619	0.77	6.75E-06	0.004	19.75	1.27E-05	0.002	0.07

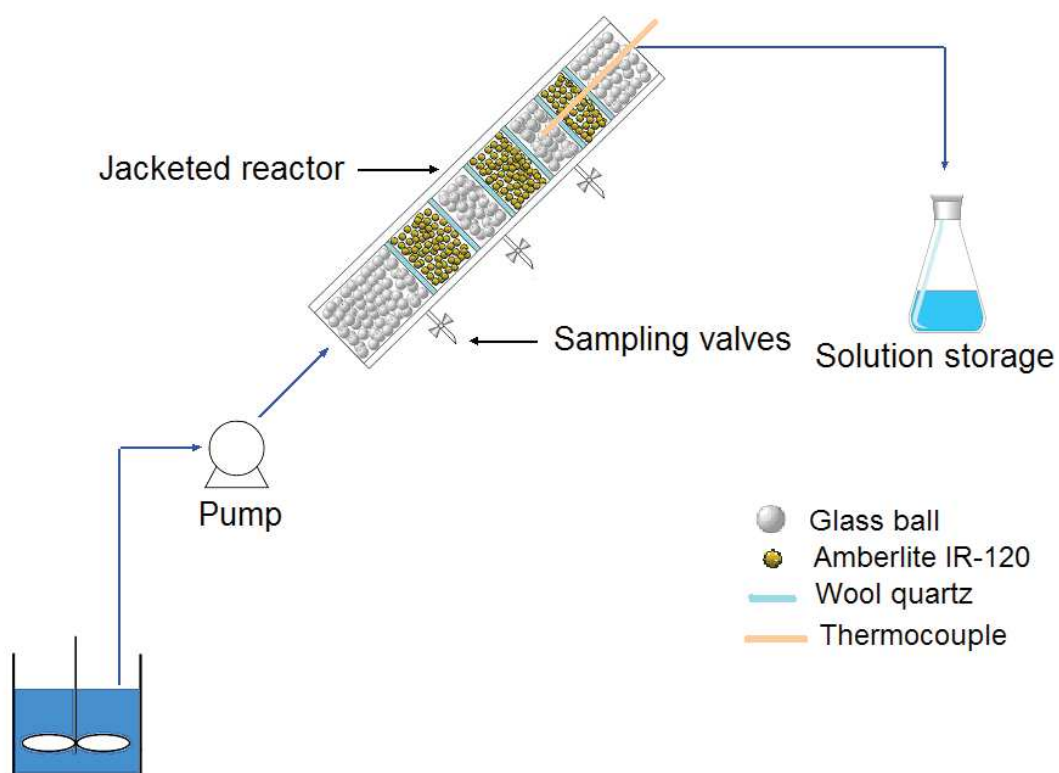
Table 10. Estimated parameters and values of standard errors at 45°C with R²:

99.40 %

Parameters	Estimated	Errors (%)
k_{ave} (l.mol ⁻¹ .s ⁻¹)	1.47 10 ⁻³	3.7
Ea (kJ/mol)	43.20	5.5

Table 11. Estimated Parameters and Values of Standard Errors at 45°C with R²:
99.20 %

Parameters	Estimated	Errors (%)
k_{ave} (l.mol ⁻¹ .s ⁻¹)	$2.10 \cdot 10^{-3}$	6.4
Ea (kJ/mol)	45.20	23.7
D_a (m ² .s ⁻¹)	$4.98 \cdot 10^{-3}$	28.5



Pre-mixing carboxylic acid and hydrogen peroxide solution

Fig. 1. Experimental scheme of the continuous fixed-bed reactor for continuous peroxycarboxylic acid production.

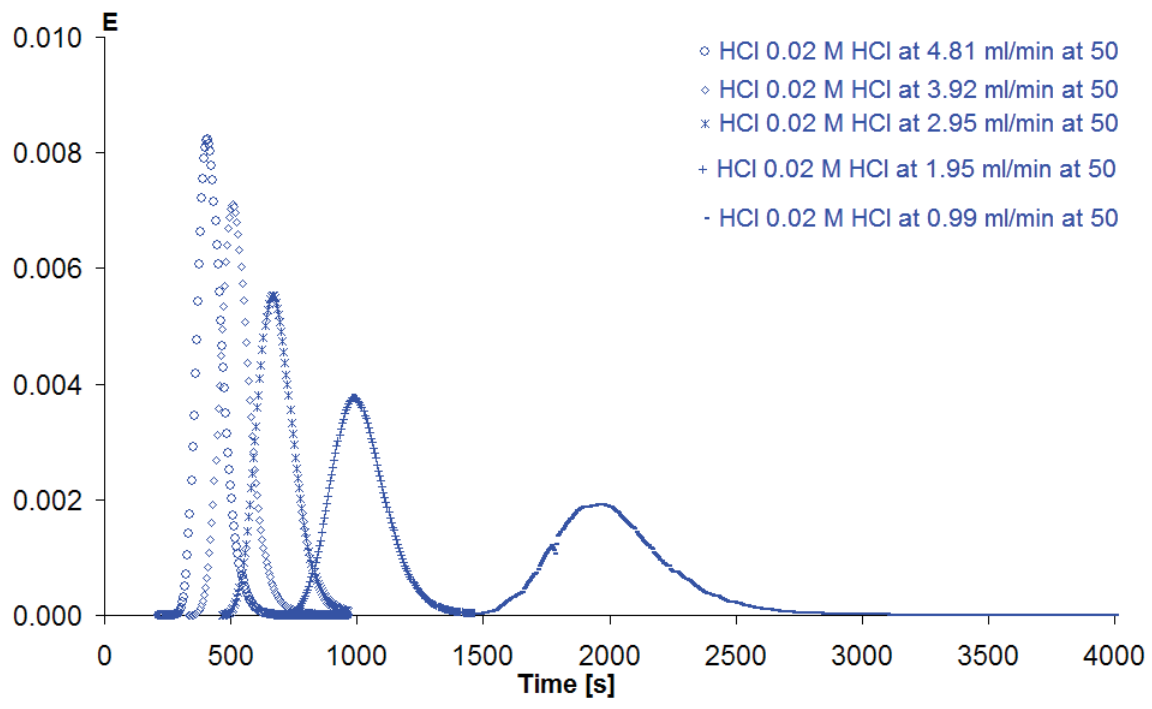


Fig.2. E-curves at 30°C by using HCl as a tracer.

Figure 3

[Click here to download Figure: Fig 3.doc](#)

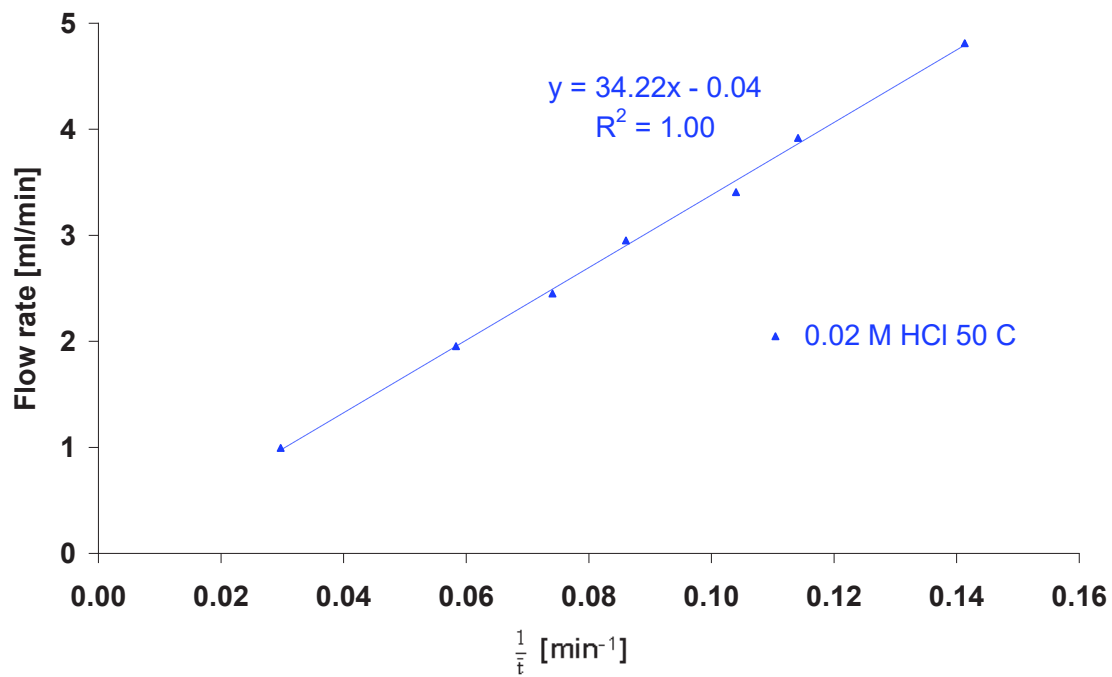


Fig. 3. Flow rate versus the inverse of the mean residence time at 50°C for reactor

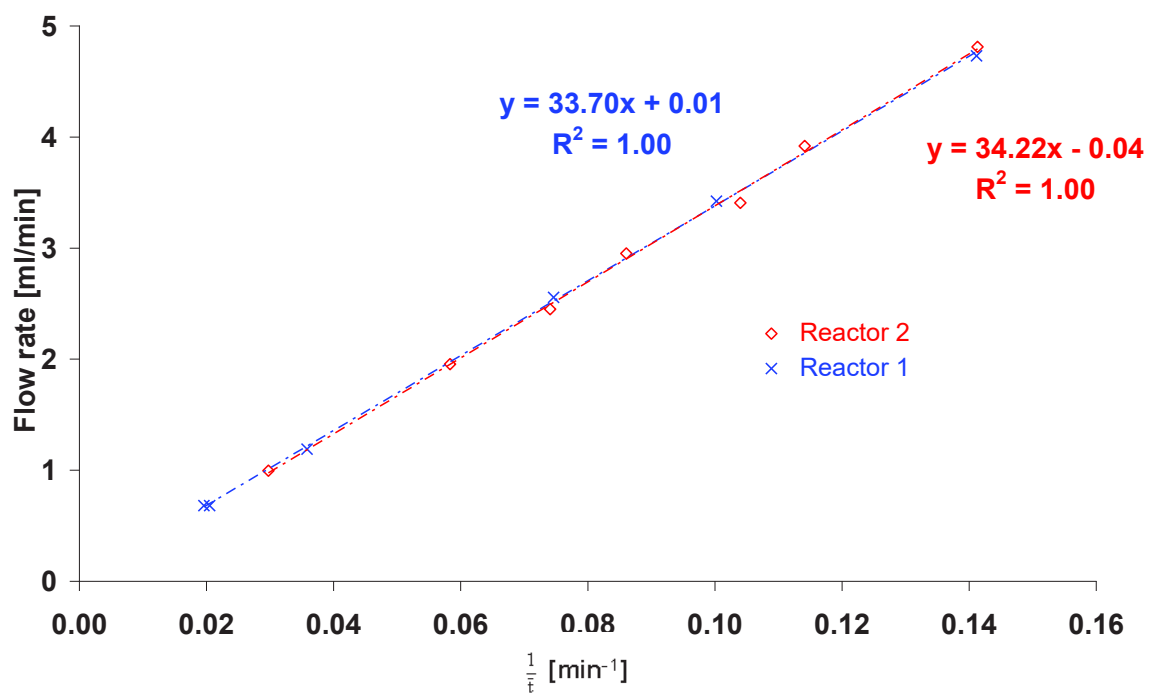


Fig. 4. Flow rate versus the inverse of the mean residence time at 50°C.

Figure 5

[Click here to download Figure: Fig 5.doc](#)

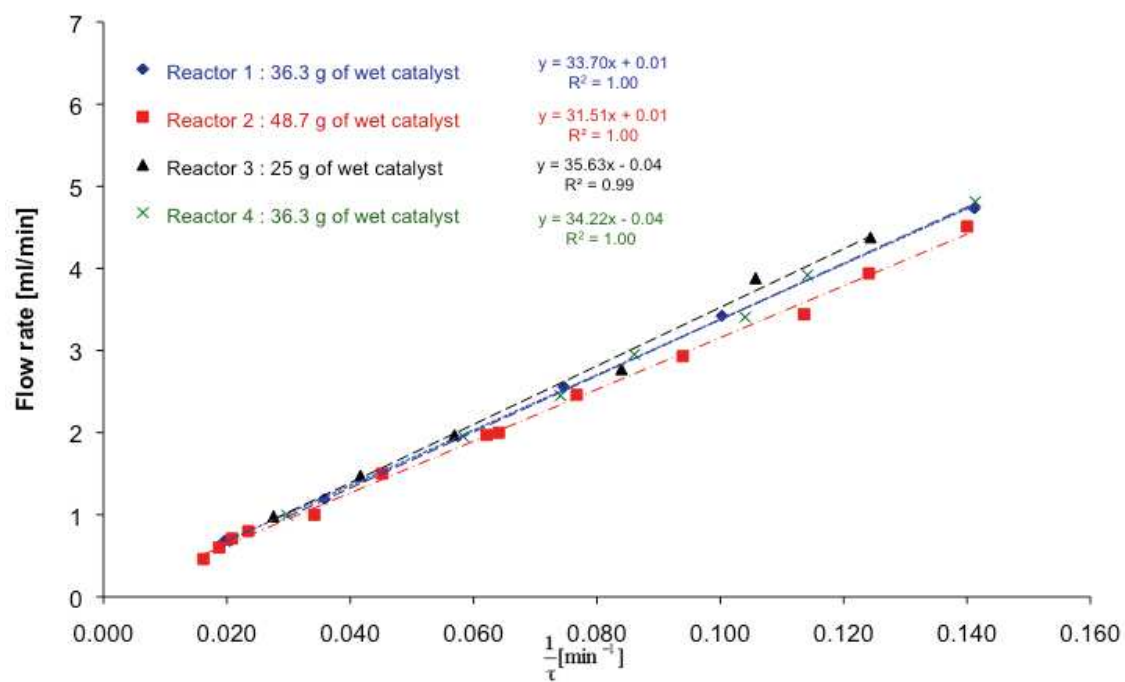


Fig. 5. Evolution of \bar{t} in different reactors.

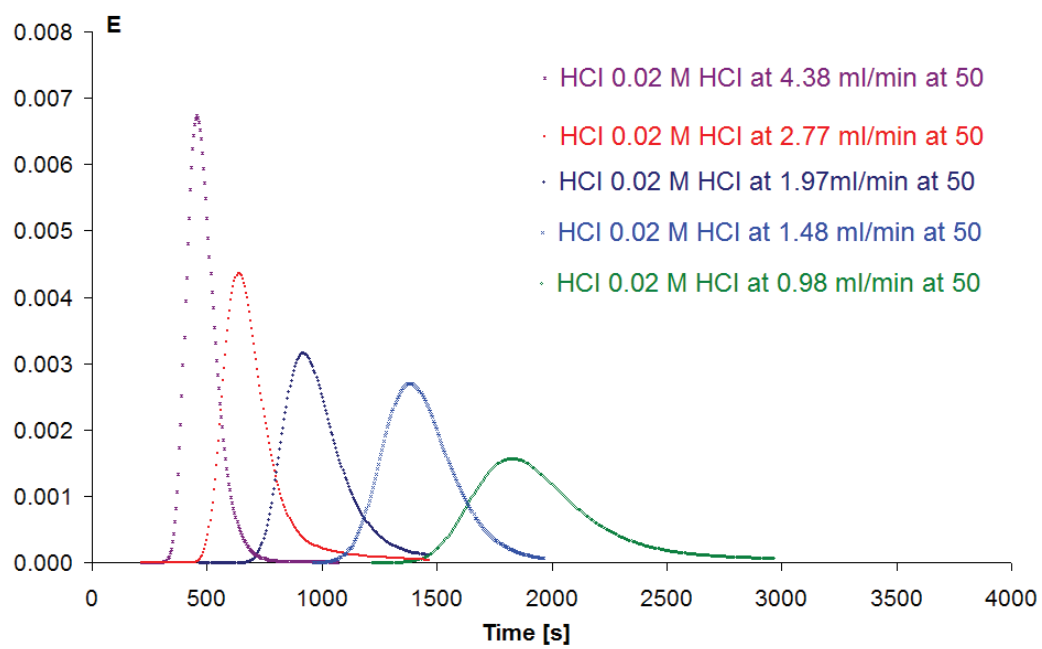


Fig. 6. E-curves for reactor 3 at different flow rates.

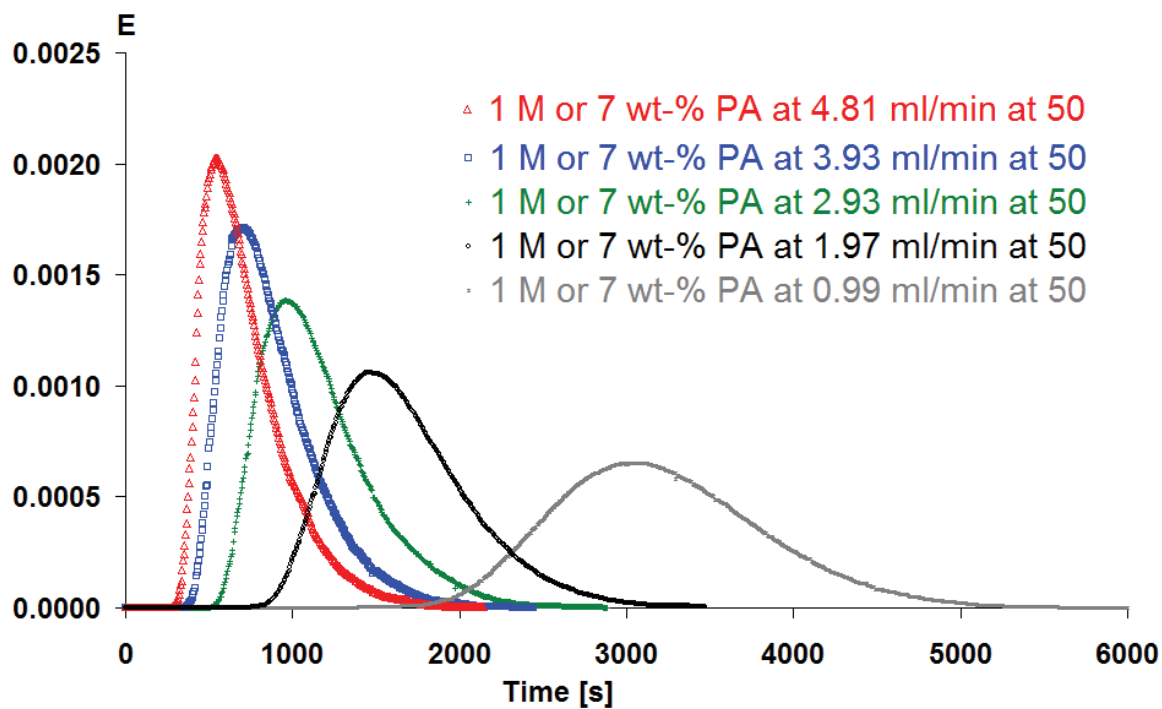


Fig. 7. E-curves for reactor 4 at 50°C using a 1 M of propionic acid solution.

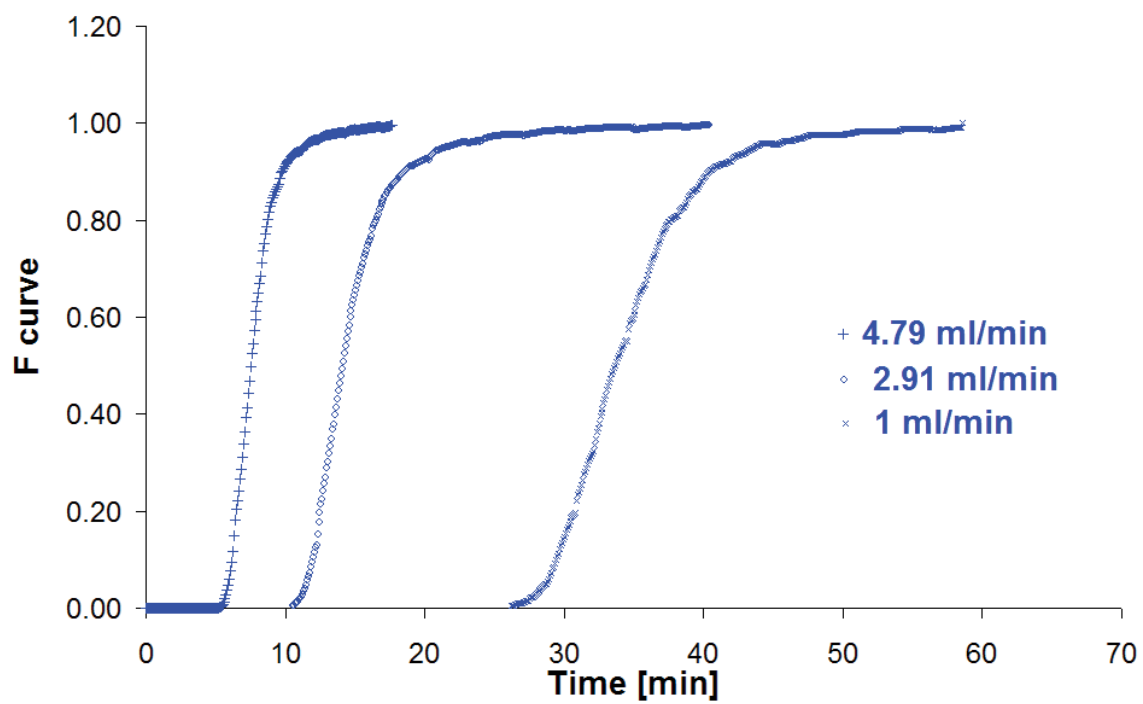


Fig. 8. F-curve for reactor 4 at 50°C with an HCl solution at 0.003 M.

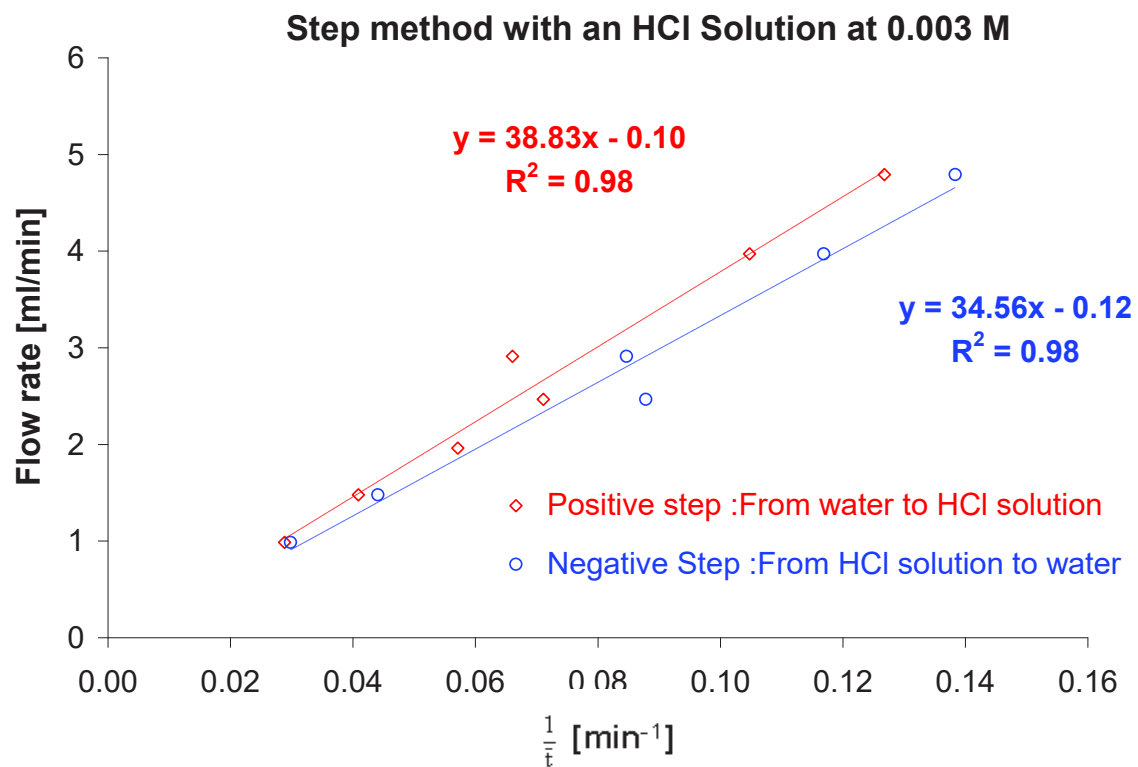


Fig. 9. Flow rate versus $\frac{1}{t}$ in the reactor 4 at 50°C.

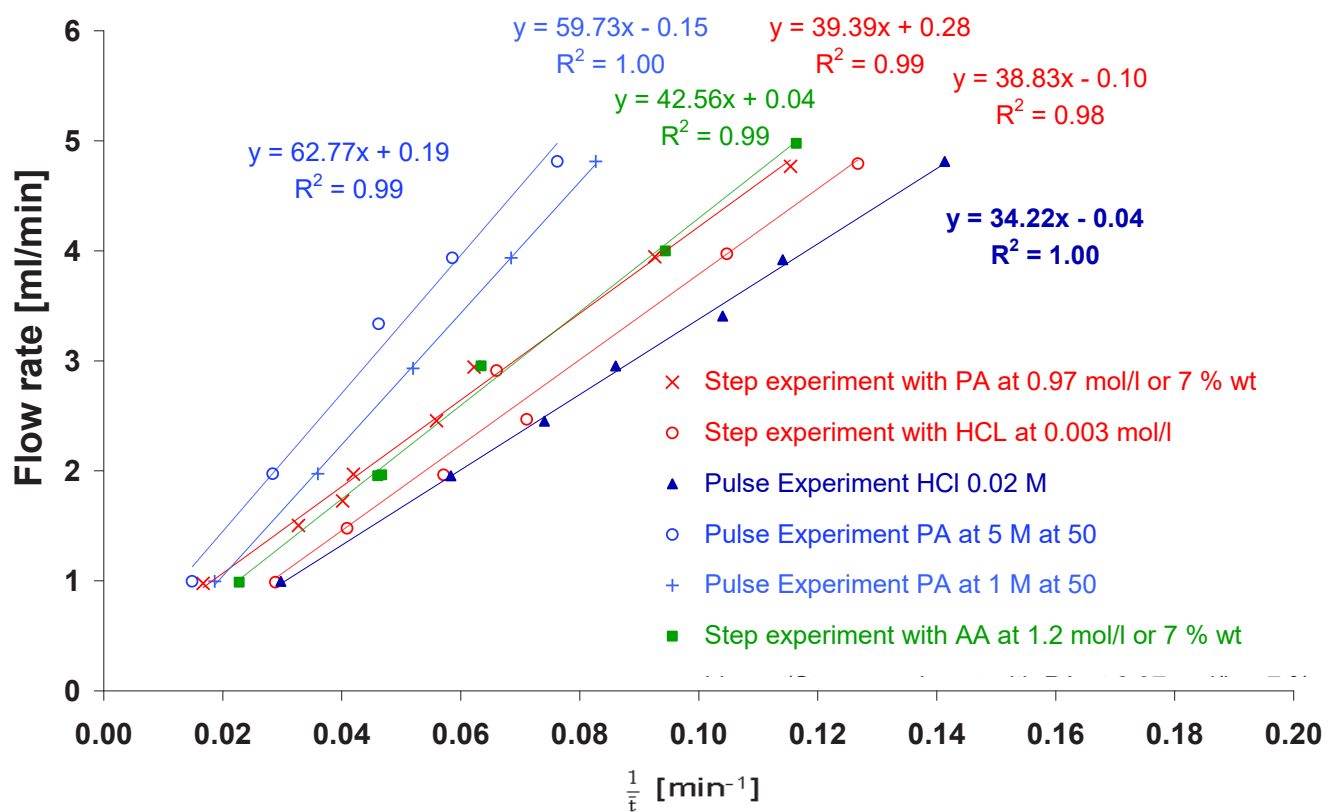


Fig. 10. Flow rate versus the reciprocal value of the mean residence time for reactor 4 at 50°C.

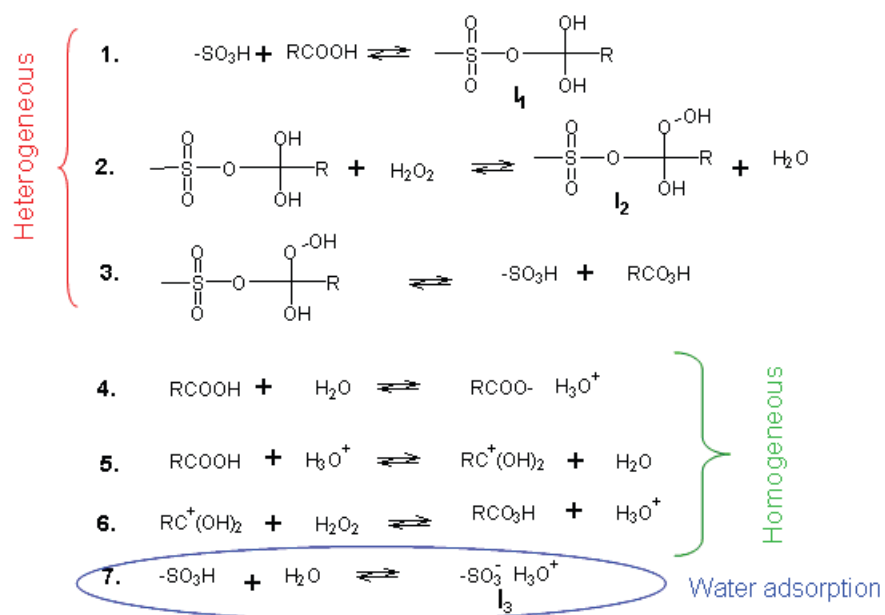


Fig. 11. Simplified mechanism for peroxydicarboxylic acid synthesis by Amberlite IR-120 in aqueous medium.

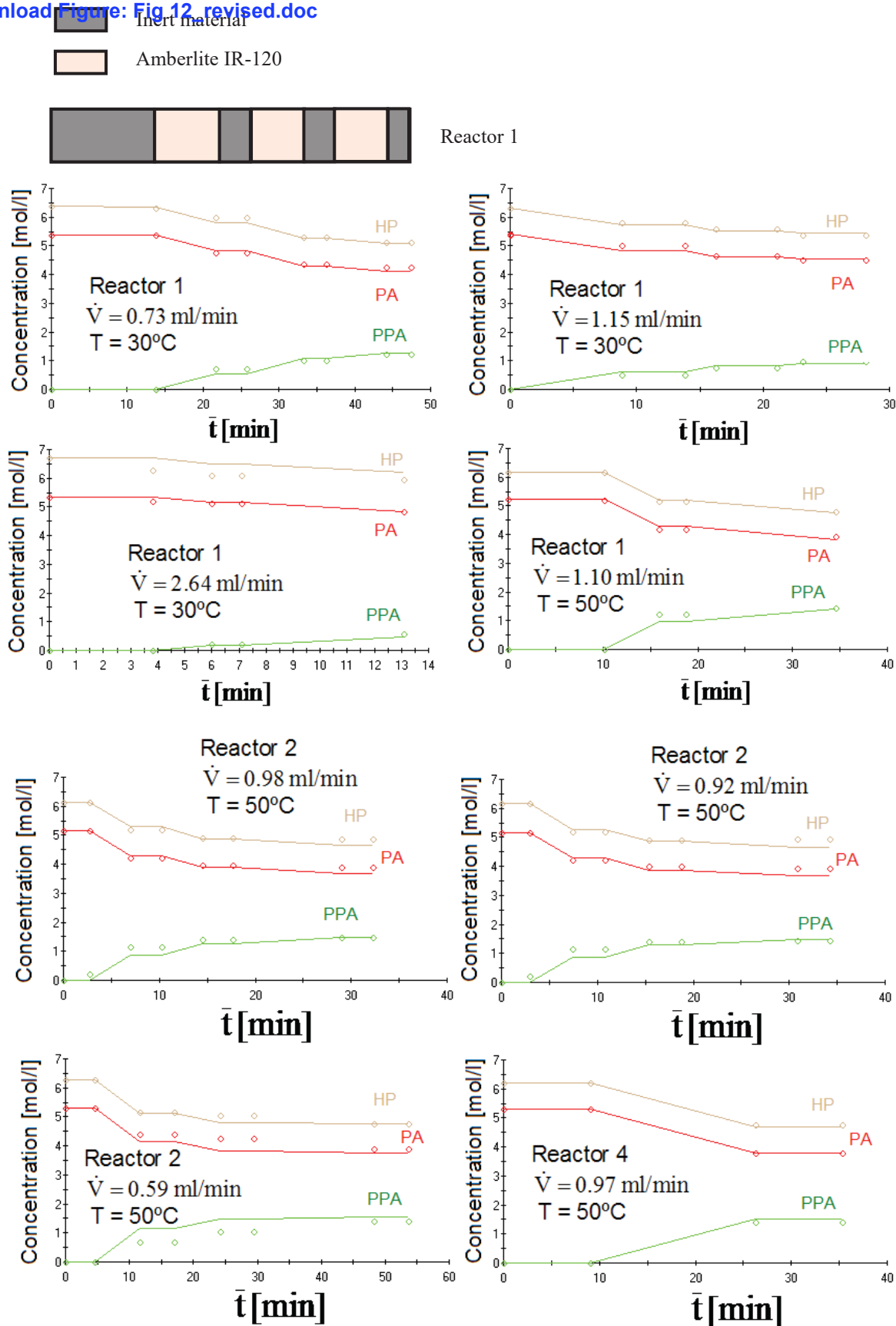


Fig. 12. Fit of the plug flow model to the perhydrolysis experiments of propionic acid.

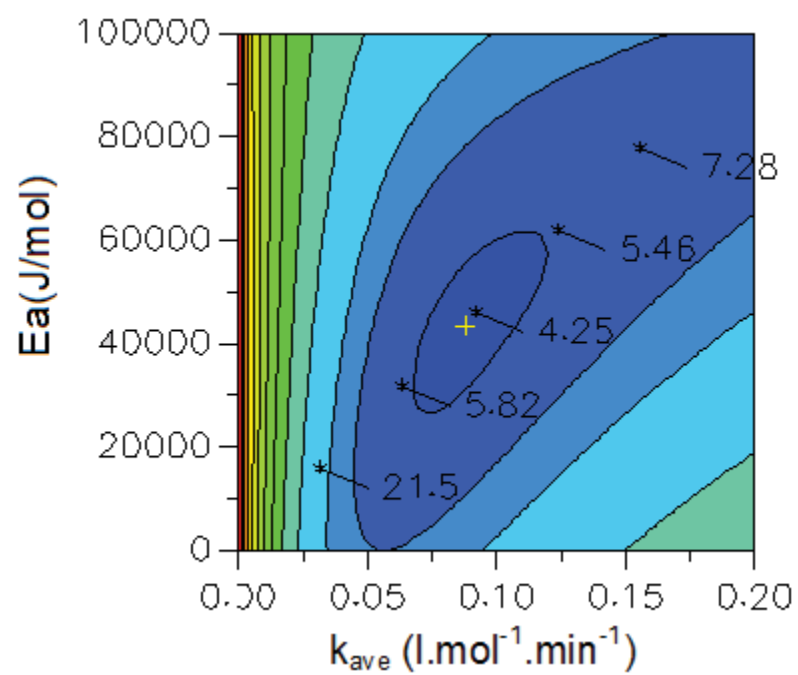


Fig. 13. Contour plot for the kinetic parameters.

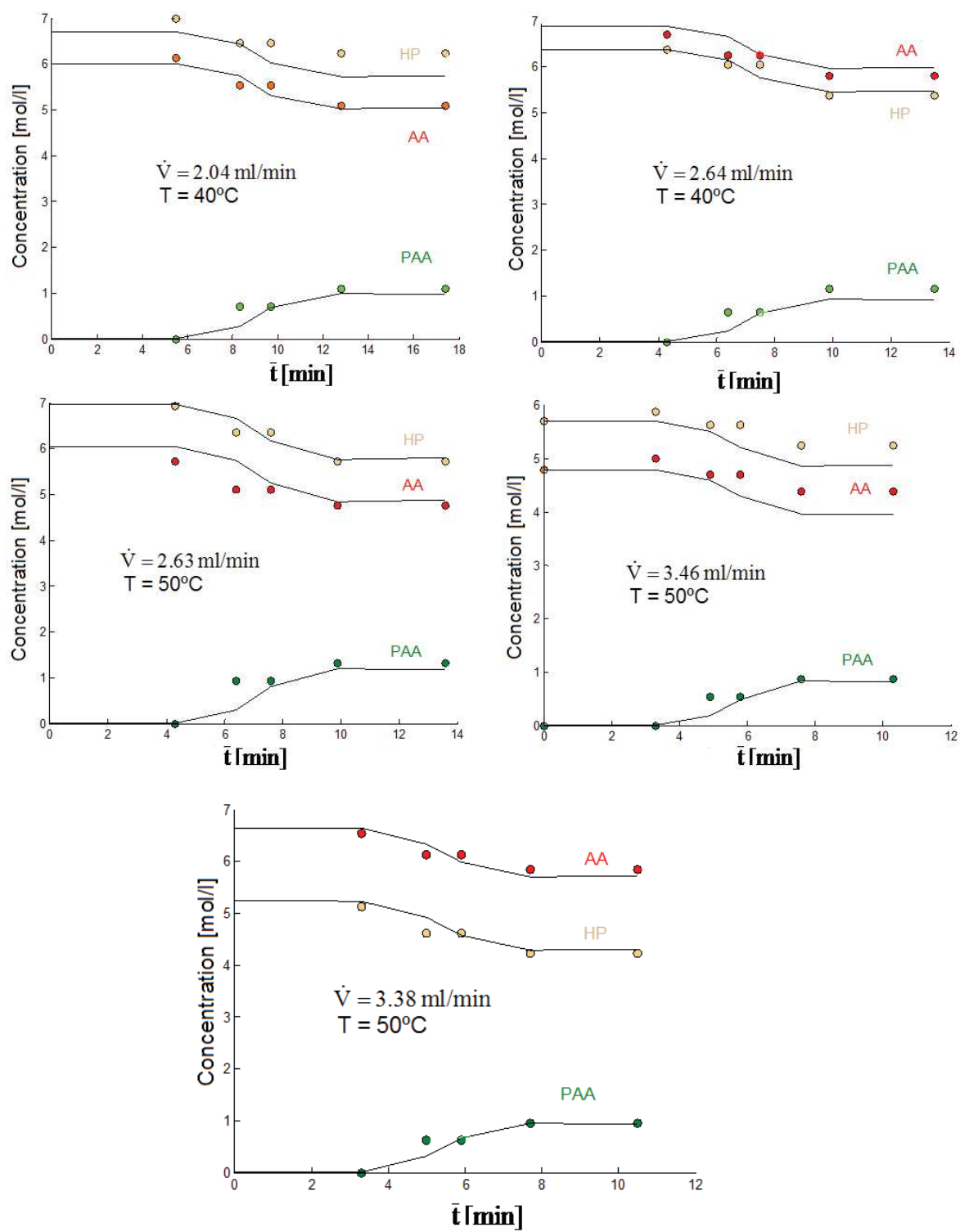


Fig. 14. Fit of the axial dispersion model to the perhydrolysis of acetic acid carried out with reactor 3.

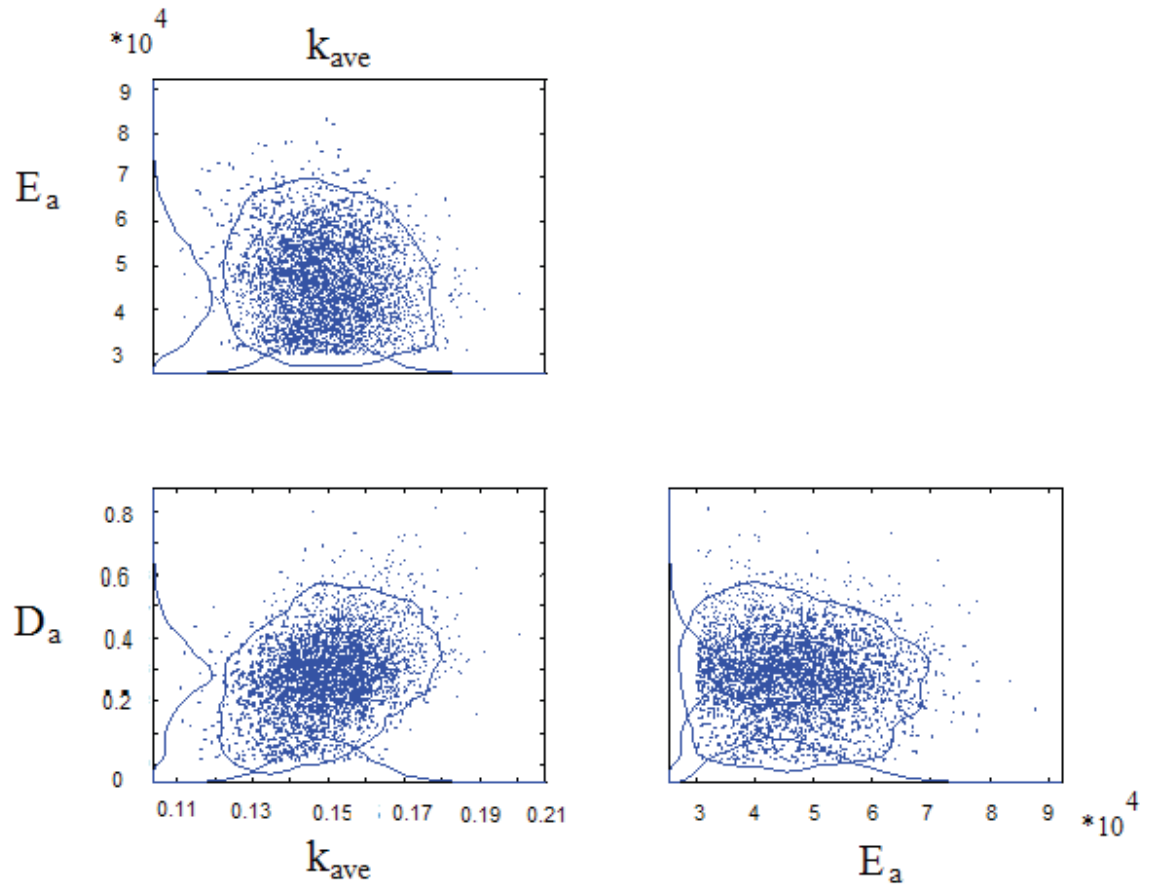


Fig. 15. Plots of the parameter sensitivity analysis (MCMC).